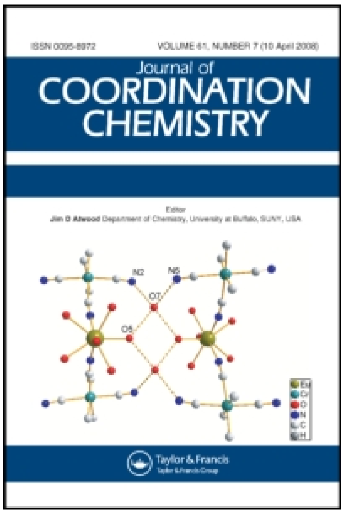

Journal of Coordination Chemistry
Publication details, including instructions for authors and subscription information:
http://www.informaworld.com/smpp/title~content=t713455674

Synthesis, structure and fluorescent properties of Cd^{II}, Zn^{II} and Ni^{II} complexes with 2-amino-6-methylbenzothiazole and 5-nitroisophthalate as ligands

Qiang Chen[a]; En-Cui Yang[a]; Run-Wen Zhang[a]; Xiu-Guang Wang[a]; Xiao-Jun Zhao[a]
[a] Key Laboratory of Molecular Structure and Materials Performance, College of Chemistry and Life Science, Tianjin Normal University, Tianjin 300387, P. R. China

To cite this Article Chen, Qiang , Yang, En-Cui , Zhang, Run-Wen , Wang, Xiu-Guang and Zhao, Xiao-Jun(2008) 'Synthesis, structure and fluorescent properties of Cd^{II}, Zn^{II} and Ni^{II} complexes with 2-amino-6-methylbenzothiazole and 5-nitroisophthalate as ligands', Journal of Coordination Chemistry, 61: 12, 1951 — 1962

To link to this Article: DOI: 10.1080/00958970701795680

URL: http://dx.doi.org/10.1080/00958970701795680

Journal of Coordination Chemistry
Vol. 61, No. 12, 20 June 2008, 1951–1962

Synthesis, structure and fluorescent properties of Cd^{II}, Zn^{II} and Ni^{II} complexes with 2-amino-6-methylbenzothiazole and 5-nitroisophthalate as ligands

QIANG CHEN, EN-CUI YANG, RUN-WEN ZHANG,
XIU-GUANG WANG and XIAO-JUN ZHAO*

Key Laboratory of Molecular Structure and Materials Performance, College of Chemistry
and Life Science, Tianjin Normal University, Tianjin 300387, P. R. China

(*Received 7 May 2007; in final form 21 June 2007*)

Three new coordination polymers, $[M(Ambt)_2(Nip)]_n$ ($M = Cd$ for **1** and Zn for **2**) and $[Ni_{0.5}(Nip)(H_2O)_2]$ (HAmbt) (**3**) (H_2Nip = 5-nitroisophthalic acid, Ambt = 2-amino-6-methylbenzothiazole), have been synthesized by hydrothermal methods and are further characterized by X-ray diffraction, IR spectra, elemental analysis, TG-DTA and fluorescence spectra. The structural analyses suggest that **1** and **2** are 1-D chains bridged by Nip anions, in which Ambt is a monodentate ligand and the carboxylate groups of Nip are monodentate and chelating bidentate. Complex **3** consists of two individual fragments, six-coordinate mononuclear Ni^{II} and HAmbt cation, in which HAmbts are encapsulated into the concave of the 2-D layer formed by mononuclear units through classic $N-H\cdots O$ hydrogen bonds. Abundant hydrogen bond interactions drive the formation of packing structure of the complexes. The three solid complexes display strong emission peaks from intraligand charge transfer similar to free Ambt at room temperature.

Keywords: 2-Amino-6-methylbenzothiazole; 5-Nitroisophthalate; Coordination polymers; Fluorescence

1. Introduction

Organic compounds containing benzothiazole and their metal complexes have optical, biological, and pharmaceutical importance used extensively as electroluminescent devices [1–3], fluorescent probes for DNA [4], corrosion inhibitors [5], anaesthetic [6], and medicines [7]. Some Pt-benzothiazole [8] and Re-benzothiazole [9] complexes have applications in electrochemical and spectroscopic fields [10, 11]. Surprisingly, there are very few reports on the synthesis and structure characterization of mixed-ligand metal complexes of 2-amino-6-methylbenzothiazole (Ambt) until now. As a biologically important reagent, Ambt and its derivatives are known for local anaesthetic action

---

*Corresponding author. Email: xiaojun_zhao15@yahoo.com.cn

Journal of Coordination Chemistry
ISSN 0095-8972 print/ISSN 1029-0389 online
DOI: 10.1080/00958970701795680

and have been developed as herbicides, fungicides and plant growth regulators [6]. In the present article, 5-nitroisophthalic acid (H_2Nip) was introduced as a ligand [12] to corporately coordinate with 3d transition metal ions (Zn^{II}, Cd^{II} and Ni^{II}) and Ambt. Herein, we present the hydrothermal synthesis, structure characterization, thermal stabilities and fluorescent properties of the obtained coordination polymers.

2. Experimental

2.1. *General materials and methods*

Ambt was purchased from Acros and other analytical-grade starting materials were obtained commercially and used as received without further purification. Doubly-deionized water was employed for synthesis. Elemental analyses of carbon, hydrogen and nitrogen were carried out with a CE-440 (Leeman-Labs) analyzer. Fourier transform (FT) IR spectra (KBr pellets) were taken on an AVATAR-370 (Nicolet) spectrometer in the range $4000-400\,\mathrm{cm}^{-1}$. Thermogravimetric analyses (TGA) were measured on a Shimadzu simultaneous DTG-60A thermal analysis instrument from room temperature to 800°C under N_2 at a heating rate of $5^{\circ}\mathrm{C\,min}^{-1}$. Fluorescence spectra of the polycrystalline powder samples were performed on a Cary Eclipse fluorescence spectrophotometer (Varian) equipped with a xenon lamp and quartz carrier at room temperature.

2.2. *Synthesis of [Cd(Ambt)$_2$(Nip)]$_n$ (1)*

An aqueous solution (10 mL) containing H_2Nip (21.0 mg, 0.1 mmol), Ambt (16.4 mg, 0.1 mmol) and $Cd(CH_3COO)_2 \cdot 4H_2O$ (53.2 mg, 0.2 mmol) was placed in a Teflon-lined stainless steel vessel (20 mL). The pH of the mixture was adjusted to 7 by slow addition of triethylamine and ethanol (1 : 3). Then it was heated to 100°C for 24 h under autogenous pressure and cooled to room temperature at the rate of $1^{\circ}\mathrm{C\,h}^{-1}$. Colorless block single crystals suitable for X-ray analysis were obtained in 61% yield (based on Ambt). IR (KBr, cm^{-1}): 3312s, 3181w, 1642m, 1529s, 1471w, 1454m, 1372m, 1339m, 1252w, 1078w, 803w, 733w, 525w. Anal. Calcd for $C_{24}H_{19}CdN_5O_6S_2$: C, 44.35; H, 2.95; N, 10.77%. Found: C, 44.65; H, 3.10; N, 10.95%.

2.3. *Synthesis of [Zn(Ambt)$_2$(Nip)]$_n$ (2)*

An aqueous solution (10 mL) containing H_2Nip (21.0 mg, 0.1 mmol), Ambt (16.4 mg, 0.1 mmol) and $ZnCl_2$ (27.2 mg, 0.2 mmol) was placed in a Parr Teflon-lined stainless steel vessel (20 mL) under autogenous pressure, heated to 140°C for 72 h and then cooled to room temperature at the rate of $5^{\circ}\mathrm{C\,h}^{-1}$. Colorless block-shaped single crystals suitable for X-ray analysis were obtained in 46% yield (based on Ambt). IR (KBr, cm^{-1}): 3302s, 3151w, 1632s, 1565s, 1529s, 1477w, 1454w, 1338s, 1257w, 1081w, 804w, 729w, 558w. Anal. Calcd for $C_{24}H_{19}ZnN_5O_6S_2$: C, 47.81; H, 3.18; N, 11.62%. Found: C, 47.65; H, 3.10; N, 11.91%.

2.4. *Synthesis of* $\{[Ni_{0.5}(Nip)(H_2O)_2]$ *(HAmbt)*$\}$ *(3)*

The synthesis conditions of **3** are similar to those of **1** except that $Ni(CH_3COO)_2 \cdot 4H_2O$ is used instead of $Cd(CH_3COO)_2 \cdot 4H_2O$. Colorless block single crystals suitable for X-ray analysis were obtained in 60.6% yield (based on Ambt). IR (KBr, cm^{-1}): 3327br, 3093w, 1609w, 1533s, 1488w, 1437m, 1355vs, 1083w, 805w, 725s, 593w. Anal. Calcd for $C_{32}H_{32}NiN_6O_{16}S_2$: C, 43.70; H, 3.67; N, 9.56%. Found: C, 43.65; H, 3.80; N, 9.81%.

2.5. *X-ray data collection and structure determinations*

Single-crystal X-ray diffraction studies of **1**–**3** were performed on a Bruker Smart 1000 CCD diffractometer equipped with a graphite crystal monochromator situated in the incident beam for data collection. The determination of unit cell parameters and data collections were performed with Mo Kα radiation ($\lambda = 0.71073$ Å) with ω scan mode. All data were corrected by semi-empirical methods using SADABS. The program SAINT [13] was used for integration of the diffraction profiles. All structures were solved by direct methods using SHELXS program of the SHELXTL-97 package and refined with SHELXL [14]. Metal atoms in all complexes were located from the *E*-maps and other non-hydrogen atoms were located in successive difference Fourier syntheses. The final refinements were performed by full matrix least-square methods with anisotropic thermal parameters for non-hydrogen atoms on F^2. The hydrogen atoms of the organic ligands were placed in calculated sites and included in the final refinement in the riding model approximation with displacement parameters derived from the parent atoms to which they were bonded. Further crystallographic data and experimental details for structural analyses of **1**–**3** are summarized in table 1.

Table 1. Crystal data and structure refinement summary for **1**–**3**.

	1	**2**	**3**
Empirical formula	$C_{24}H_{19}CdN_5O_6S_2$	$C_{24}H_{19}ZnN_5O_6S_2$	$C_{32}H_{32}NiN_6O_{16}S_2$
Mr	649.96	602.93	879.46
Crystal size (mm^3)	0.24 × 0.23 × 0.20	0.25 × 0.23 × 0.20	0.24 × 0.08 × 0.07
Crystal system	Monoclinic	Monoclinic	Monoclinic
Space group	$C2/c$	$C2/c$	$P2(1)/c$
a (Å)	23.7901(19)	23.4304(18)	19.421(3)
b (Å)	13.4449(11)	14.1127(11)	13.7017(18)
c (Å)	17.1952(14)	16.2938(12)	6.8957(9)
β (°)	98.3100(10)	93.0350(10)	95.706(2)
V (Å)^3	5442.2(8)	5380.3(7)	1825.9(4)
Z	8	8	4
ρ_{Calcd} ($g\,cm^{-3}$)	1.587	1.489	1.600
μ (mm^{-1})	1.003	1.116	0.729
$F(000)$	2608	2464	908
Range of h, k, l	−25/28, −15/17, −20/20	−27/26, −16/16, −13/19	−21/23, −16/16, −8/7
Total/independent reflections	14409/4775	14436/4732	9769/3207
Parameters	345	345	260
R_{int}	0.0262	0.0357	0.0563
R^a, R_w^b	0.0278, 0.0378	0.0371, 0.0625	0.0462, 0.0856
GOF^c	1.011	1.029	1.024
Residuals/e (Å^{-3})	0.673, −0.271	0.566, −0.345	0.357, −0.380

$^aR = \Sigma\|F_o| - |F_c\|/\Sigma|F_o|$. $^bR_w = [\sum[w(F_o^2 - F_c^2)^2]/\sum w(F_o^2)^2]^{1/2}$. $^c\mathrm{GOF} = \{\sum[w(F_o^2 - F_c^2)^2]/(n-p)\}^{1/2}$.

Table 2. Selected bond lengths (Å) and angles (°) for **1**.

Bond lengths			
Cd(1)–O(1)	2.427(2)	Cd(1)–O(2)	2.3213(19)
Cd(1)–N(3)	2.274(2)	Cd(1)–O(4)#1	2.247(2)
Cd(1)–N(1)	2.249(2)	O(4)–Cd(1)#2	2.247(2)
Bond angles			
O(4)#1–Cd(1)–N(1)	106.47(9)	O(4)#1–Cd(1)–N(3)	91.91(8)
N(1)–Cd(1)–N(3)	116.47(9)	O(4)#1–Cd(1)–O(2)	148.80(8)
N(1)–Cd(1)–O(2)	92.55(8)	N(3)–Cd(1)–O(2)	101.61(8)
O(4)#1–Cd(1)–O(1)	95.31(8)	N(1)–Cd(1)–O(1)	136.08(8)
N(3)–Cd(1)–O(1)	100.00(8)	O(2)–Cd(1)–O(1)	54.93(7)
N(1)–Cd(1)–C(17)	115.76(9)	N(3)–Cd(1)–C(17)	101.81(9)
O(4)–Cd(1)–C(17)	122.36(9)	O(2)–Cd(1)–C(17)	27.48(7)
O(1)–Cd(1)–C(17)	27.46(7)		

Symmetry codes: #1: $x, -y+2, z-1/2$; #2: $x, -y+2, z+1/2$.

3. Results and discussion

3.1. *Preparations of complexes 1–3*

Coordination polymers **1**–**3** were isolated by similar hydrothermal methods. The molar ratio of reactants for **1**–**3** are all 1 : 1 : 2 (H_2Nip: Ambt: metal salt), indicating that the molar ratio of the starting materials have little effect on the final crystalline product. In contrast, the reaction temperature and pH of the mixture play important roles for formation of the final products. Both **1** and **3** are obtained at 100°C, while **2** is obtained at 140°C. Attempts to synthesize **2** at 100°C failed. Deprotonation of H_2Nip is necessary to facilitate coordination; considering the basicity of Ambt, no measures were taken to control the pH of the reaction mixture and **2** and **3** were obtained with complete deprotonation of H_2Nip. However, **1** requires a more basic environment and the pH was controlled by mixed triethylamine and ethanol solution. Appropriate reaction temperature and basic medium are key factors for the formation of the complexes.

3.2. *Structure description of [Cd(Ambt)$_2$(Nip)]$_n$ (1)*

Single-crystal X-ray diffraction analysis reveals that **1** is an infinite one-dimensional (1-D) chain bridged by Nip anions. The fundamental unit of **1** contains one Cd^{II}, two Ambt molecules and a Nip dianion. As depicted in figure 1(a), each Cd^{II} is five-coordinate in a distorted square-pyramidal geometry. The basal plane of each metal ion is surrounded by three oxygen atoms from two different Nip anions and one nitrogen atom from Ambt ligand with Cd–O and Cd–N distances varying from 2.249(2) to 2.427(2) Å. The maximum deviation of the four atoms to the least-squares plane is 0.1864 Å. The apical position is occupied by a nitrogen atom from the other Ambt with Cd–N of 2.274(2) Å. Two neighboring five-coordinate Cd^{II} ions are joined via two carboxylate groups of Nip in chelating bidentate and monodentate fashion to generate an infinite chain with Cd $\cdots$ Cd separation of 9.8582(7) Å (figure 1b). The Cd1–O1 bond length in chelating bidentate carboxylate is slightly longer than that of Cd1–O2, suggesting an asymmetric chelating bidentate binding. Both Cd–O bond lengths in the

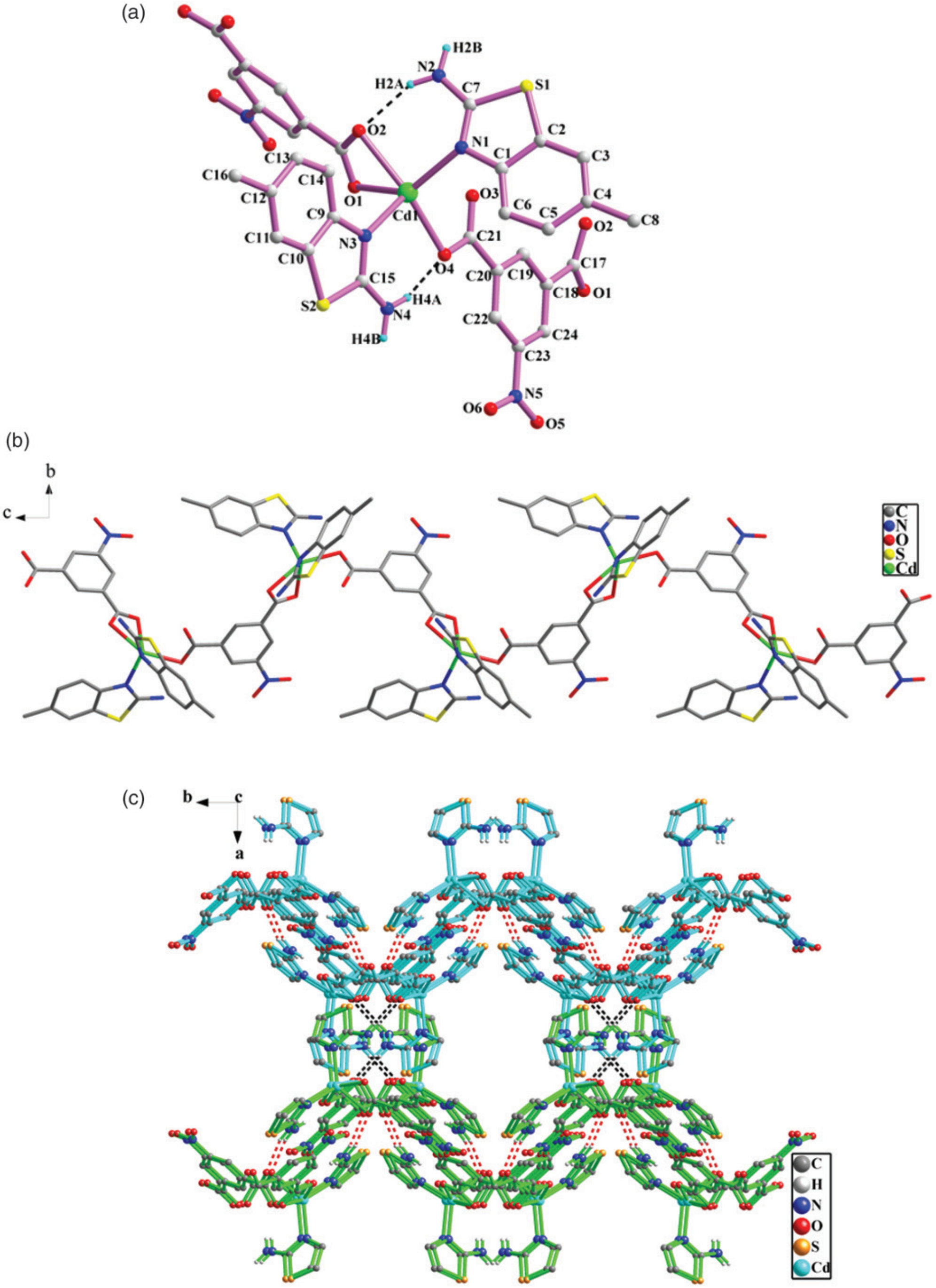

Figure 1. (a) Cd^{II} coordination environment of **1** with atom labeling of the asymmetric unit (only H atoms involved in H-bonding are included). (b) An infinite 1-D chain of **1** bridged by Nip anions. (c) 3-D packing structure of **1** (methyl group and benzene ring of Ambt are omitted for clarity).

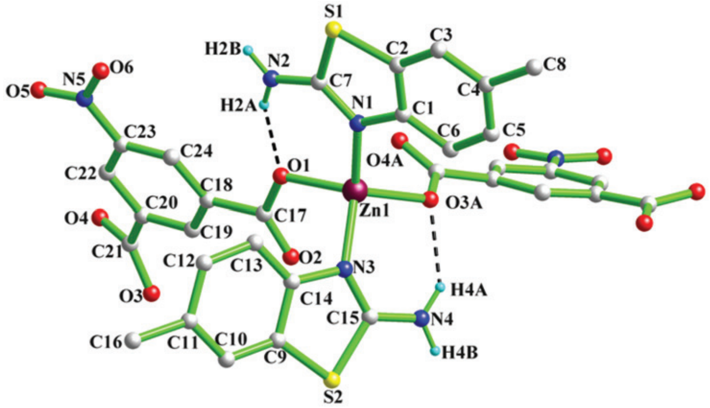

Figure 2. Zn^{II} coordination sphere of **2** (only H atoms involved in H-bonding are included).

Table 3. Selected bond lengths (Å) and angles (°) for **2**.

Bond lengths			
Zn(1)–O(3)#1	1.954(2)	Zn(1)–O(1)	1.9628(19)
Zn(1)–N(1)	2.019(2)	Zn(1)–N(3)	2.031(3)
Bond angles			
O(3)#1–Zn(1)–O(1)	126.78(9)	O(3)#1–Zn(1)–N(1)	109.20(9)
O(1)–Zn(1)–N(1)	100.41(9)	O(3)#1–Zn(1)–N(3)	101.80(10)
O(1)–Zn(1)–N(3)	104.00(10)	N(1)–Zn(1)–N(3)	115.30(10)

Symmetry codes: #1: x, $-y$, $z+1/2$.

chelating bidentate binding mode are longer than monodentate Cd1–O4. Both Ambt ligands coordinate through the thiazole ring nitrogen to Cd^{II}. As a hydrogen bond donor, the amino group of Ambt displays intrachain N–H···O H-bonding with carboxylate oxygen of Nip, which further consolidates the 1-D chain-like structure of **1**.

Adjacent 1-D chains are linked together into a 2-D wave-like layer by N–H···O H-bonding interactions between the amino group of Ambt and carboxylate oxygen atoms of Nip. These 2-D layers are further stacked into 3-D supramolecular networks (figure 1c and table 5).

3.3. *Structure description of* $[Zn(Ambt)_2(Nip)]_n$ *(2)*

Similar to **1**, **2** is also a 1-D infinite chain connected by Nip anions. Due to the analogous structure of the two complexes (see figure S1–S2 in the supporting materials), we will only discuss the differences of **2** from **1**. The Zn^{II} in the asymmetric unit of **2** is surrounded by two thiazole nitrogen atoms and two carboxylate oxygen atoms from separate Nip anions, forming a distort tetrahedron with the Zn–N and Zn–O bond lengths varying from 1.954(2) to 2.031(3) Å (figure 2 and table 3). The carboxylate groups in Nip dianion are monodentate, connecting the adjacent Zn^{II} ions into a 1-D infinite chain with the Zn···Zn separation of 9.653 Å.

3.4. *Structure description of {[$Ni_{0.5}(Nip)(H_2O)_2$]} (HAmbt) (3)*

Different from both **1** and **2**, complex **3** consists of two fragments, a centrosymmetrical mononuclear $[Ni_{0.5}(Nip)(H_2O)_2]^-$ anion and a protonated Ambt cation for charge-compensation. As shown in figure 3(a), the central Ni^{II} ion in the mononuclear unit is six-coordinate with four oxygens from four independent waters and two carboxylate oxygen atoms from two separate Nip dianions. The Ni–O bond lengths vary from 2.016(2) to 2.092(3) Å (see table 4) in a slightly distorted octahedron. The Nip anion is monodentate through one of its carboxylate oxygens. Within the mononuclear unit, weak O(7)–H(7A) $\cdots$ O(1) interactions between coordinated water molecule and carboxylate oxygen of Nip (see table 5) help consolidate the mononuclear fragment.

Adjacent mononuclear fragments are joined by H-bonding interactions between the coordinated water molecules and oxygen atoms of carboxylate in Nip, extending infinitely in two directions to generate an interdigitated 2-D layer as shown in figure 3b. Although phenyl-rings are present in **3**, only weak $\pi \cdots \pi$ stacking interactions were observed in the 2-D layer with the minimum centroid-to-centroid distances of 3.737 Å. Furthermore, the HAmbt cations are shallowly encapsulated into the concave of the layer by the H-bonding interactions between the amino group and carboxylate group anions (see table 5).

3.5. *Infrared spectra*

In the IR spectra of the three complexes, the peaks at 3181, 1471 and 733 cm^{-1} for **1**, 3151, 1477 and 729 cm^{-1} for **2**, and 3093, 1488 and 725 cm^{-1} for **3** correspond to framework vibrations of benzothiazole ring [15]. The strong peaks at 3312 cm^{-1} for **1** and 3302 cm^{-1} for **2** are NH_2 stretch vibrations in Ambt. For **3**, the observed broad band at 3327 cm^{-1} is the stretch of coordinated water and amino of Ambt. The C=N stretching vibrations of thiazole rings are at 1529 cm^{-1} for **1** and **2** and 1533 cm^{-1} for **3**, and the peaks from 1078 to 1083 cm^{-1} result from ν(C–S–C) vibration of the thiazole ring. New peaks at 525, 558 and 593 cm^{-1} for **1**–**3**, respectively, indicate that nitrogen of the thiazole ring coordinates monodentate [16, 17], in agreement with the crystal structure. The absence of the characteristic peak at ca 1700 cm^{-1} for the protonated carboxylate groups indicates the complete deprotonation of H_2Nip. The asymmetric and symmetric C=O stretching vibration bands of carboxylate groups at 1642 and 1454 cm^{-1} for **1**, 1565 and 1338 cm^{-1} for **2**, and 1609 and 1355 cm^{-1} for **3** suggest diverse coordination modes of the Nip dianion in monodentate and chelating bidentate fashions [18].

3.6. *Thermogravimetric analysis*

Due to the similar chain-shaped structure of **1** and **2**, **2** and **3** were chosen to examine the thermal stabilities. As shown in figure 4, **2** has three consecutive weight-loss processes. The first weight-loss stage with an endothermic peak began at 169°C and ended at 334°C. The weight loss of this stage is 26.6%, corresponding to decomposition of one Ambt (Calcd 27.2%). The second weight-loss process of 26.3% (Calcd 27.2%) was from 334°C to 510°C with an obviously exothermic effect. This stage was assigned

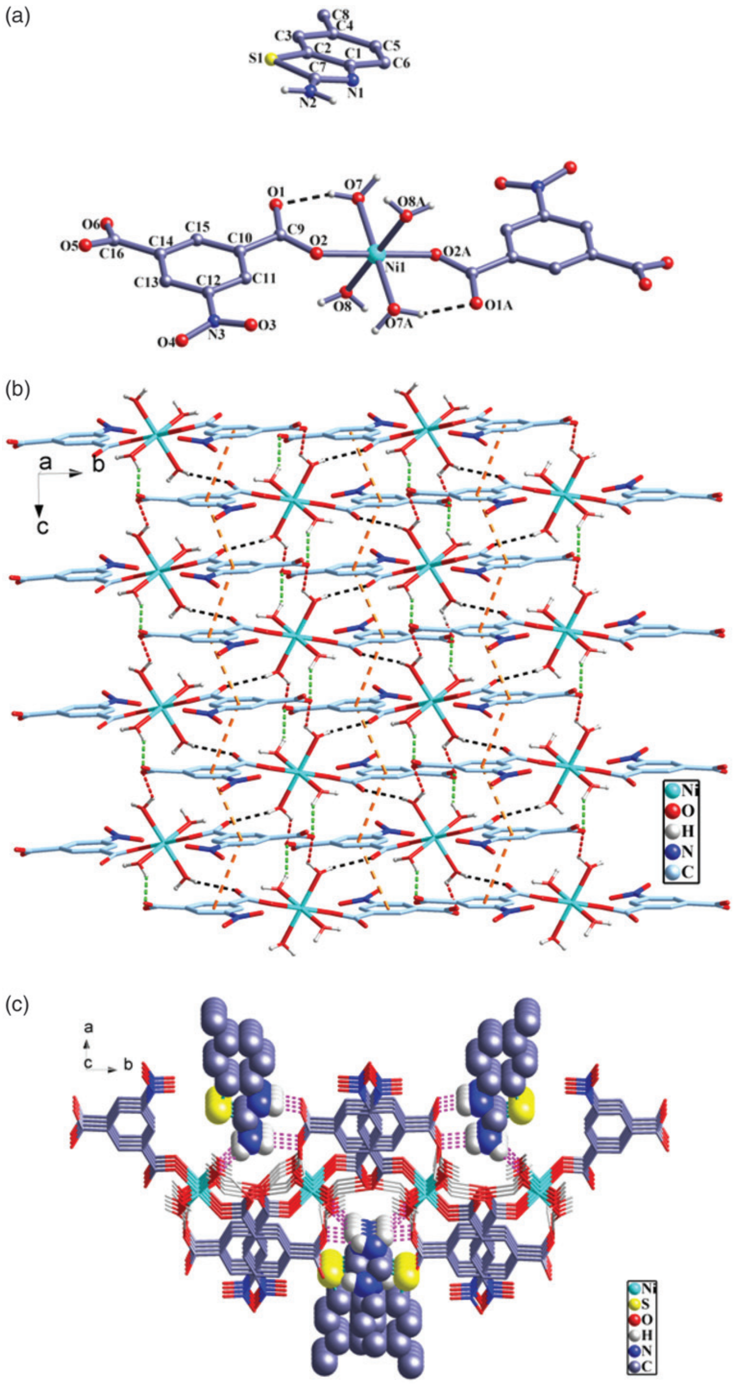

Figure 3. (a) Ni^{II} coordination environment of **3** with atom labeling of the asymmetric unit (H atoms of aromatic ring are omitted for clarity; symmetry operation A: $-x+1$, $-y+2$, $-z+1$). (b) 2-D supramolecular layer of **3** formed by mononuclear Ni fragments (only H atoms involved in H-bonding are included). (c) The HAmbt binding with the 2-D layer by H-bonding interactions.

Table 4. Selected bond lengths (Å) and angles (°) for **3**.

Bond lengths			
Ni(1)–O(2)	2.016(2)	Ni(1)–O(7)	2.069(2)
Ni(1)–O(8)	2.092(3)		
Bond angles			
O(2)–Ni(1)–O(2)#1	180.000(1)	O(2)–Ni(1)–O(7)	89.76(9)
O(2)#1–Ni(1)–O(7)	90.24(10)	O(2)–Ni(1)–O(7)#1	90.24(10)
O(2)#1–Ni(1)–O(7)#1	89.76(9)	O(7)–Ni(1)–O(7)#1	180.0
O(2)–Ni(1)–O(8)	93.31(10)	O(2)#1–Ni(1)–O(8)	86.69(10)
O(7)–Ni(1)–O(8)	92.17(11)	O(7)#1–Ni(1)–O(8)	87.83(11)
O(2)–Ni(1)–O(8)#1	86.69(10)	O(2)#1–Ni(1)–O(8)#1	93.31(10)
O(7)–Ni(1)–O(8)#1	87.83(11)	O(7)#1–Ni(1)–O(8)#1	92.17(11)
O(8)–Ni(1)–O(8)#1	180.00(1)		

Symmetry codes: #1: $-x+1$, $-y+2$, $-z+1$.

Table 5. Hydrogen bond geometries for **1**–**3**.

D–H···A	D–H	D···A (Å)	H···A (Å)	D–H···A (°)
1				
N(2)–H(2A)···O(2)	0.860	2.873(4)	2.071	154
N(2)–H(2B)···O(3)#1	0.860	2.826(4)	2.030	153
N(4)–H(4A)···O(4)	0.860	2.722(4)	1.896	160
N(4)–H(4B)···O(1)#2	0.860	2.821(3)	2.012	156
2				
N(2)–H(2A)···O(1)	0.860	2.750(3)	1.957	152
N(2)–H(2B)···O(4)#1	0.860	2.779(4)	1.948	162
N(4)–H(4A)···O(3)	0.860	2.862(4)	2.134	142
N(4)–H(4B)···O(2)#2	0.860	2.790(4)	1.963	161
3				
O(7)–H(7A)···O(1)	0.820	2.617(3)	1.856	153
O(7)–H(7B)···O(6)#1	0.850	2.776(4)	1.993	152
O(8)–H(8′)···O(6)#2	0.820	2.810(5)	2.245	126
O(8)–H(8″)···O(1)#1	0.850	2.886(4)	2.172	141
N(1)–H(1)···O(5)	0.860	2.574(4)	1.729	167
N(2)–H(2A)···O(6)	0.860	2.933(4)	2.084	169
N(2)–H(2B)···O(7)#3	0.860	2.923(4)	2.116	156

Symmetry codes: for **1**: #1 $-x$, $1-y$, $1-z$; #2 $1/2-x$, $1/2-y$, $1-z$; for **2**: #1 $1/2-x$, $1/2-y$, $-z$; #2 $-x$, $1-y$, $-z$; for **3**: #1 $1-x$, $y+1/2$, $-z+1/2$; #2 x, $-y+3/2$, $z-1/2$; #3 $1-x$, $1-y$, $1-z$.

to loss of another Ambt ligand. Upon further heating, slow weight loss occurred until 650°C, also with an exothermic peak, ascribed to simultaneous decomposition of two Nip anions (Calcd 34.7%; Obs. 34.1%).

Different from **2**, the framework of **3** lost coordinated water molecules from 136°C to 158°C (Obs. 8.4%; Calcd 8.2%). Then continuous weight loss occurred from 170°C to 415°C, which could be attributed to decomposition of Nip anions (Obs. 47.27%; Calcd 47.53%). Upon further heating, the hydrogen-bonded HAmbt cations were decomposed in the range 415–556°C (Obs. 37.18%; Calcd 37.53%).

3.7. *Fluorescent properties*

The fluorescence properties of **1**–**3** were examined in the solid state at room temperature. As shown in figure 5, both **1** and **2** show strong emission at 360 nm

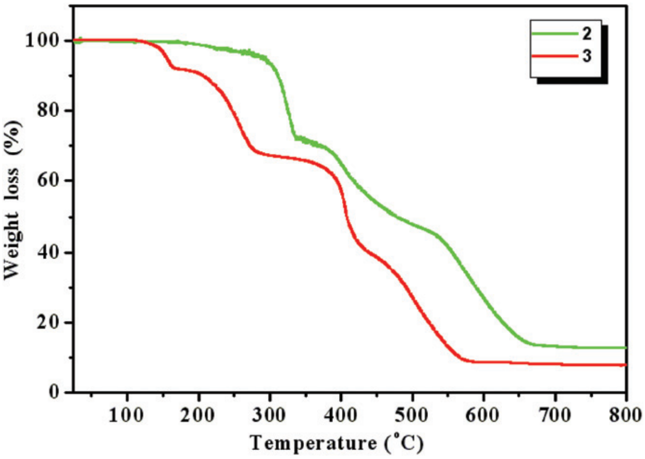

Figure 4. TG curves of **2** and **3**.

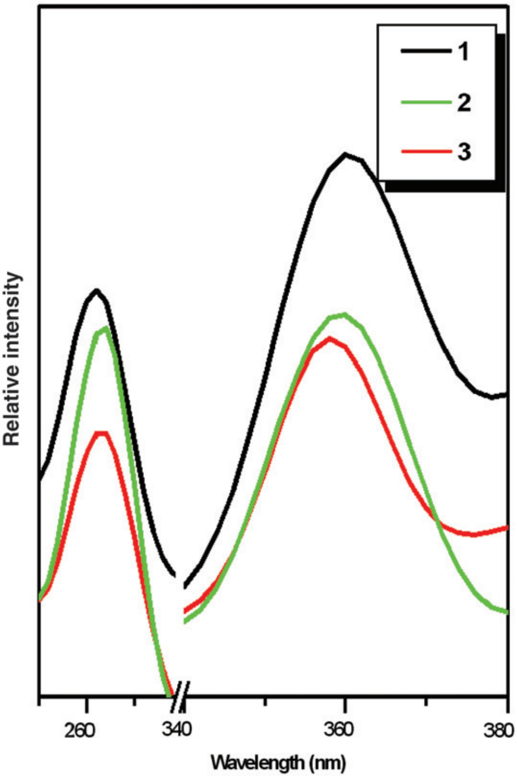

Figure 5. Emission and excitation spectra of **1**–**3** in the solid state at room temperature.

upon excitation at 264 nm, although relative fluorescence intensities are somewhat different. In contrast, **3** displayed an emission band centered at 358 nm upon excitation at 262 nm. Since the free Ambt ligand exhibits a similar emission at 355 nm upon excitation at 260 nm under the same conditions, the fluorescent behavior of the three complexes can be assigned to intraligand charge transfer. The slight red-shift, compared with the free Ambt ligand, is attributed to both deprotonation of the H_2Nip and the coordination of Ambt and carboxylate groups to metal ions.

4. Conclusion

In this research, three new mixed-ligand Cd^{II}, Zn^{II} and Ni^{II} complexes, $[M(Ambt)_2(Nip)]_n$ (M = Cd for **1** and Zn for **2**) and $[Ni_{0.5}(Nip)(H_2O)_2]$ (HAmbt) **3**, were successfully isolated by hydrothermal synthesis. Both **1** and **2** exhibit a 1-D infinite chain structure and further develop into a 3-D supramolecular network by hydrogen-bond interactions, although the carboxylate groups display two different binding modes. In contrast, **3** is a hydrogen-bonded supramolecule consisting of mononuclear Ni^{II} and dissociative HAmbt fragments. Owing to intraligand charge transfer, the three solid complexes show similar fluorescent emission spectra at room temperature.

Supplementary material

Crystallographic data (excluding structure factors) for the crystal structures reported in this paper have been deposited with the Cambridge Crystallographic Data Center (CCDC Nos. 646107–646109). This material can be obtained free of charge via www.ccdc.cam.ac.uk/conts/retrieving.html (or from the CCDC, 12 Union Road, Cambridge CB2 1EZ, UK; fax: +44 1223 336033; e-mail: deposit@ccdc.cam.ac.uk). The structural figures of **2** are available free of charge via the Internet.

Acknowledgements

The present work was jointly supported by the National Natural Science Foundation of China (20571056), (20703030), National Key Fundamental Research Project of China (2005CCA01200), Natural Science Foundation of Tianjin (06YFJMJC03900) and the Tianjin Educational Committee (20060501).

References

[1] X.H. Zhang, O.Y. Wong, Z.Q. Gao, C.S. Lee, H.L. Kwong, S.T. Lee, S.K. Wu. *Mater. Sci. Eng. B*, **85**, 182 (2001).
[2] R.M.F. Batista, S.P.G. Costa, E.L. Malheiro, M. Belsley, M.M.M. Raposo. *Tetrahedron*, **63**, 4258 (2007).
[3] W.N. Leng, Y.M. Zhou, Q.H. Xu, J.Z. Liu. *Polymer*, **42**, 9253 (2001).
[4] V.B. Kovalska, K.D. Volkova, M.Y. Losytskyy, O.I. Tolmachev, A.O. Balanda, S.M. Yarmoluk. *Spectrochim. Acta, Part A*, **65**, 27 (2006).
[5] J.C. Marconato, L.O. Bulhoes, M.L. Temperini. *Electrochim. Acta*, **43**, 771 (1998).
[6] H.W. He, L.P. Mens, L.M. Hu, Z.J. Liu. *Chin. J. Pestic. Sci.*, **4**, 14 (2002).
[7] J.V.N. Vara-Prasad, A. Panapoulous, J.R. Rubin. *Tetrahedron Lett.*, **41**, 4065 (2000).

[8] X.-F. He, C.M. Vogels, A. Decken, S. Westcott. *Polyhedron*, **23**, 155 (2004).
[9] R. Czerwieniec, A. Kapturkiewicz, J. Lipkowski, J. Nowacki. *Inorg. Chim. Acta*, **358**, 2701 (2005).
[10] S.K. Hadjikakou, M. Kubicki. *Polyhedron*, **19**, 2231 (2000).
[11] X.Y. Chen, F.J. Femia, J.W. Babich, J. Zubieta. *Inorg. Chim. Acta*, **314**, 91 (2001).
[12] (a) C.G. Zhang, J. Zhang, Z.F. Chen, Z.J. Guo, R.G. Xiong, X.Z. You. *J. Coord. Chem.*, **55**, 835 (2002). (b) L. Gao, B.J. Zhao, Z. Shi, S.H. Feng. *Inorg. Chem. Commun.*, **6**, 1249 (2003). (c) B. Moulton, H. Abourahma, M.W. Bradner, J. Lu, G.J. Mcmanus, M.J. Zaworotko. *Chem. Commun.*, 1342 (2003).
[13] A.X.S. Bruker. *SAINT Software Reference Manual*, Madison, WI (1998).
[14] G.M. Sheldrick. *SHELXTL NT Version 5.1 Program for Solution and Refinement of Crystal Structures*, University of Göttingen, Germany (1997).
[15] Q. Ying. *Dyes and Pigments* (2006) doi:10.1016 (in press).
[16] S. Saydam, E. Yilmaz. *Spectrochim. Acta, Part A*, **63**, 506 (2006).
[17] R. Castro, J.A. Garcia-Vazquez, J. Romero, A. Sousa. *Polyhedron*, **12**, 2241 (1993).
[18] (a) G.B. Deacon, R.J. Phillips. *Coord. Chem. Rev.*, **33**, 227 (1980). (b) K. Nakamoto. *Infrared and Raman Spectra of Inorganic and Coordination Compounds*, Wiley, New York (1986).